

Comparative Assessment of PID, Fuzzy Logic and ANFIS Controllers in an Automatic Voltage Regulator of A Power System

Shwan Ch. Abdulla^{1, 2*} 

¹Electrical Engineering Department, College of Engineering, University of Sulaimani, Sulaimani, Iraq

²Computer Engineering Department, College of Engineering, Komar University of Science and Technology, Sulaimani, Iraq

E-mail: shwan.abdullah@univsul.edu.iq

Received: September 24, 2022

Revised: November 07, 2022

Accepted: November 13, 2022

Abstract— A comparative study and performance analysis of three different controllers - namely proportional-integral-derivative (PID), PD-like fuzzy logic and adaptive neuro fuzzy inference system (ANFIS) - utilized to control the output voltage of an automatic voltage regulator (AVR) of a power system are carried out. The obtained results show that the PID controller is capable of rejecting simultaneous disturbance signals effectively with zero steady-state error (SSE). However, it is not robust to unexpected parameter changes of the system. On the other hand, the fuzzy logic controller shows the ability to resist changes in the system parameters. Nonetheless, it exhibits both an increase of 12.5% in the SSE and fluctuations in disturbance rejection test. On the contrary, the ANFIS controller shows: i) superior performance and ii) robustness to disturbance signals and changes in the system parameters compared to the other two controllers. For these reasons, we believe that utilization of an ANFIS controller will not only promote safety, but also reliability of the AVR in power systems.

Keywords— PID controller; Fuzzy logic controller; Adaptive neuro fuzzy inference system; Automatic voltage regulator; Feedback control.

1. INTRODUCTION

Automatic voltage regulator (AVR) is usually used in power systems to provide simultaneous voltage control and keep a terminal voltage of generators constant at a specific level. Since power systems deal with high voltages, any fluctuations in the terminal voltage may lead to serious problems. For this reason, the security of a power system depends on the stability of the AVR. Sometimes, it is difficult to attain a stable and fast response of the AVR due to load variations, high inductance of windings of the generator, and insulation failure due to voltage fluctuations. Hence, enhancement of the AVR performance is extremely important. This can be achieved by utilizing an effective control algorithm to eliminate the above-mentioned issues.

Different control strategies are reported in the literature to control the AVR systems, such as proportional-integral-derivative (PID) [1-3], fuzzy logic [4, 5] and adaptive and predictive control [6-9]. To improve the performance of the controller, various closed-loop control approaches in combination with optimization techniques have been introduced [2, 10-12]. The fractional order PID - optimized by cuckoo search algorithm [13] and particle swarm optimization (PSO) algorithm [14] - is introduced. Fuzzy logic in combination with genetic algorithm (GA) is introduced to find the optimal parameter values of the PID controller [15]. In addition, Fuzzy logic together with a modified PSO is utilized to obtain the optimal controller's gain values and attain an on-line optimized transient response [16, 17].

Further, Fuzzy logic and PID controllers are implemented to balance the overall system generation against different burdens and losses in the AVR system [18]. In addition to PID and fuzzy logic controllers (FLCs), adaptive neuro fuzzy inference system (ANFIS) is utilized in an attempt to reduce the low frequency oscillations in the system [6]. ANFIS is also used to provide an online tuning of PID controllers by training the ANFIS controller with optimized PID data [19]. Further, model predictive control and H-infinity based control paradigms are presented to handle the uncertainties of the AVR parameters [7, 8]. Furthermore, the neural network (NN) predictive controller optimized by the imperialist competitive algorithm is introduced to overcome the fluctuation in the terminal voltage of the AVR system [9].

The feedback closed-loop response of AVR system has some shortages in terms of time-domain indices. These indicators are used to assess the closed-loop response of the system. Ideally, the response requires lower values of settling time, rise time and overshoots with minimum steady-state error (SSE) [20]. On the other hand, unexpected changes in system parameters threaten the stability and security of the power system. In addition, due to system disturbances, the electrical oscillations may occur for a long time and result in system instability [21]. Hence, in power systems, choosing an appropriate control strategy to cope with unexpected system changes and disturbances is of high importance.

The PID controller is well-known for its trouble-free implementation and simple configuration. However, the PID is affected by problems such as nonlinearities in the system and requires re-tuning to controller's parameters [22]. The FLC is usually utilized for its simplicity, effectiveness, low cost, robustness and its ability to overcome nonlinearity in complex systems [5]. The ANFIS is a very effective approach in modeling complex and nonlinear systems with high precision. It combines the accurate learning and adaptive capabilities of NN with the fast learning capability of the fuzzy logic [21]. These three controllers, i.e., PID, FLC and ANFIS have been widely used in different engineering applications [23-25]. In addition, these controllers are extensively utilized in various control approaches to control the AVR in power systems [1, 6, 26-29]. However, the literature lacks a detailed study of the three controllers in terms of stability and robustness to unexpected disturbances and changes in system parameters in AVR systems. In this research, the controllers, namely PID, FLC and ANFIS are employed in a closed-loop control approach to control an AVR system, and the performance of each controller is evaluated. The time response of the controllers - in terms of rise time (T_r), settling time (T_s), delay time (T_d) and SSE - is recorded and analyzed. Additionally, to examine the ability of each controller to cope with unexpected disturbances, a disturbance test is conducted. Further, to test the robustness of each controller against unexpected changes in system parameters, each controller is tested with different system parameters. The controller of the best performance is suggested to provide stability and reliability of power systems.

This research paper is organized into six sections. Section 2 represents the description of the AVR system. Section 3 describes the implementation and the results of the three controllers; PID, FLC and ANFIS. The disturbance rejection test is conducted in section 4. The robustness of the controllers - against changes in system parameters - is tested in section 5. Finally, the conclusion is presented in section 6.

2. DESCRIPTION OF THE AVR SYSTEM

AVR is an essential module used to maintain the terminal voltage of any power generator system. The AVR system continuously monitors the terminal voltage of the power generator and adjusts the exciter voltage to maintain the operation of the generator within predetermined limits. The AVR system - as shown in Fig. 1 - consists of four main parts: the amplifier, exciter, generator and sensor. To model and determine the transfer function of each part, linearization is necessary by ignoring the nonlinearities and the saturation of each component. The major time constant of each component must also be considered [22]. The transfer function of the amplifier is considered as:

$$G_a = \frac{K_a}{1+\tau_a s} \quad (1)$$

where K_a represents the amplifier's gain, while τ_a represents the time constant of the amplifier's model. The standard range of the gain K_a is between 10 and 400, while the standard range of the time constant τ_a is between 0.02 and 0.1 s.

Also, the transfer function of the exciter is represented as:

$$G_e = \frac{K_e}{1+\tau_e s} \quad (2)$$

where K_e represents the exciter's gain, and τ_e represents the time constant of the exciter's model. The standard range of the gain K_e is between 1 and 400, while the standard range of the time constant τ_e is between 0.4 and 1 s.

Similarly, the transfer function of a linearized generator model is represented by:

$$G_g = \frac{K_g}{1+\tau_g s} \quad (3)$$

where K_g represents the generator's gain, and τ_g represents the time constant of the generator's model. The standard range of the gain K_g is between 0.7 and 1, whereas the standard range of the time constant τ_g is between 1 and 2 s.

Finally, the transfer function of a sensor model is represented by:

$$G_s = \frac{K_s}{1+\tau_s s} \quad (4)$$

where K_s represents the sensor's gain, and τ_s represents the time constant of the sensor. The standard range of the gain K_s is 1, while the standard range of the time constant τ_s is between 0.001 and 0.06 s.

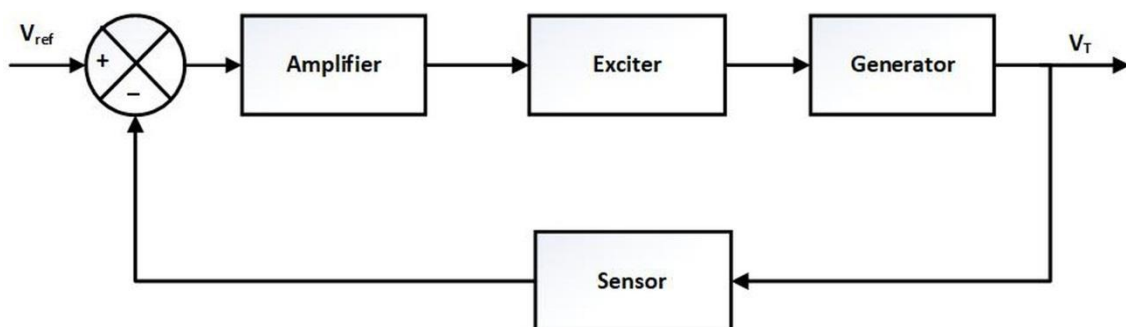


Fig. 1. Block diagram of the AVR system.

In this article, the values of different parameters of the AVR system are considered as $K_a = 10$, $\tau_a = 0.1$, $K_e = 1$, $\tau_e = 0.4$, $K_g = 1$, $\tau_g = 1$, $K_s = 1$ and $\tau_s = 0.01$. The closed-loop transfer function of the AVR system without a controller is represented as [15]:

$$G_{AVR}(s) = \frac{0.1s+10}{0.0004s^4 + 0.0454s^3 + 0.555s^2 + 1.51s + 11} \quad (5)$$

The closed-loop response of the AVR system without a controller can be seen in Fig. 2. From the closed-loop transfer function $G_{AVR}(s)$, it is clear that the system possesses one zero at -100, two complex poles at $-0.5285+4.6649i$ and $-0.5285-4.6649i$ and two real poles at -98.81 and -12.62. The closed-loop response of the AVR system without a controller is highly oscillatory and diverges from the desired steady-state value of 1. The oscillatory behavior records a maximum overshoot of 1.5 with rise time = 0.26 s, settling time = 7.01 s and steady-state value of 0.9. This oscillatory behavior is unacceptable, as the operating range of the power system is of the order of 100 kV, and it affects the stability and the security of the power system [20]. In this work, to improve the transient and the steady-state behavior of the AVR system, three different controllers are utilized, tested and analyzed.

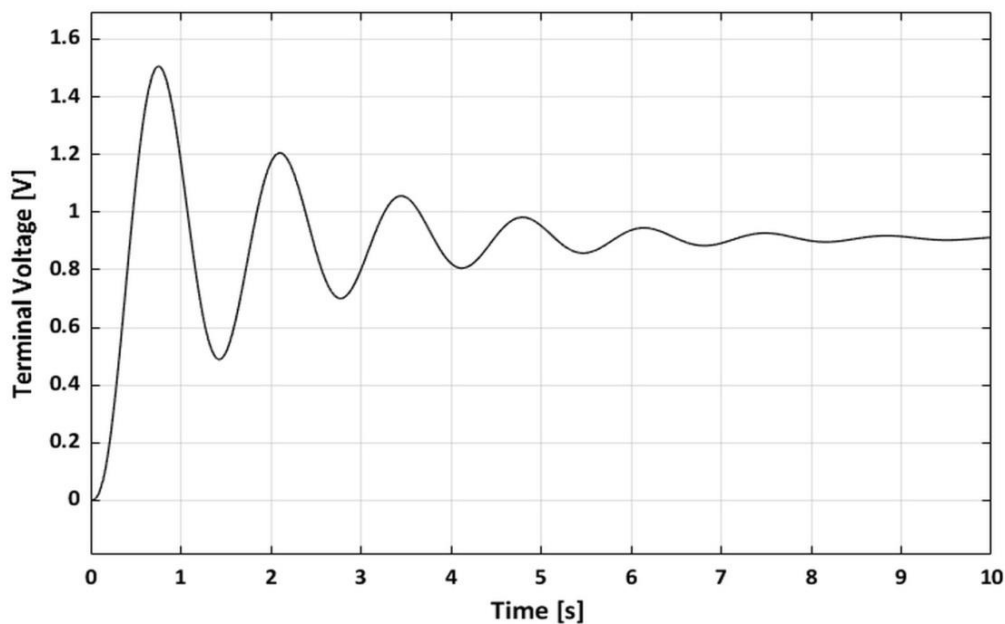


Fig. 2. Closed-loop response of the AVR without controller.

3. CONTROLLERS

In this research work, three different controllers are used with the AVR system. These are: PID, PD-like Fuzzy logic and ANFIS controllers. The performance of each controller is recorded and evaluated as discussed in the following subsections.

3.1. PID Controller

In this section, a PID controller is used to control the output voltage of the AVR system to follow a desired unity step input reference voltage in a closed-loop control approach. The closed-loop control approach is exhibited in Fig. 3. The PID controller transfer function is described as:

$$G_{PID}(s) = K_p + \frac{K_i}{s} + K_d s \quad (6)$$

where K_p , K_i , and K_d are the proportional coefficient, integral coefficient and derivative coefficient, respectively.

To tune the PID controller and obtain the desired performance of the system, different tuning methods can be used such as heuristic, model-based and rule-based tuning. In this work, to obtain an acceptable and precise performance of the controller, the values of the PID controller are obtained using the PID tuner facility provided by Matlab/Simulink software. The tuning process of the PID is performed to obtain fast system response with minimum overshoot and zero steady-state error. The obtained PID values are $P= 0.12174$, $I= 0.10296$ and $D= 0.01668$.

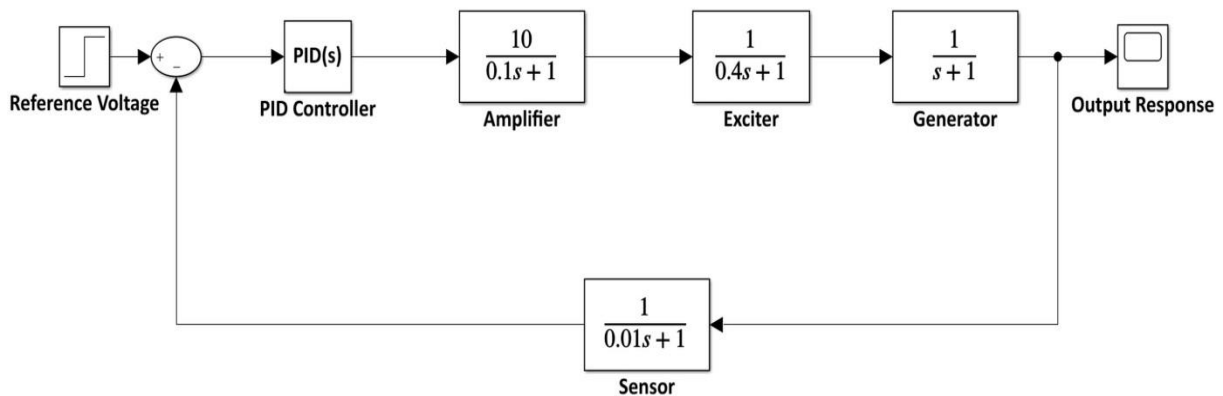


Fig. 3. The closed-loop control approach using the PID controller.

3.1.1. Results

The step response of the PID closed-loop control approach is shown in Fig. 4. It is clear from the response that the system is stable and the SSE in the terminal voltage is zero. The delay time (T_d) is 0.87 s, rise time (T_r) is 1.54 s, and the settling time (T_s) is 3.50 s.

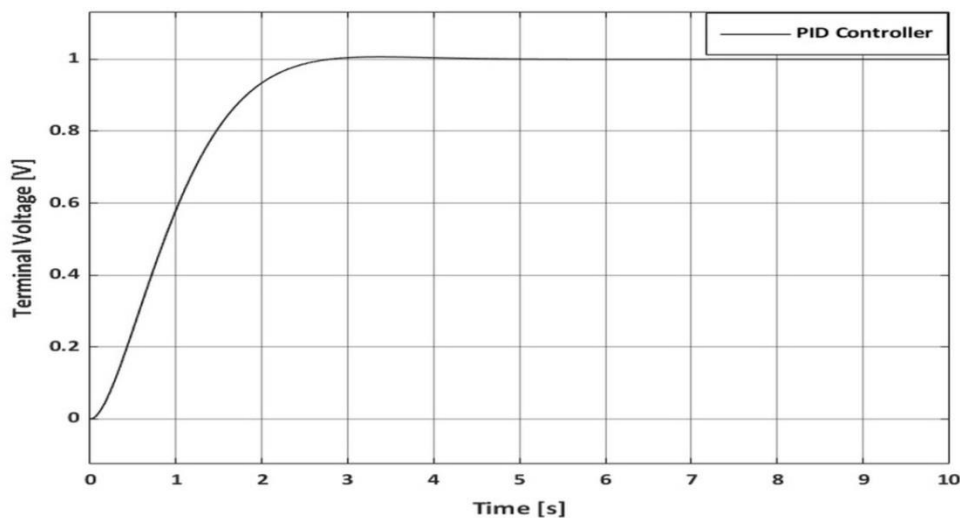


Fig. 4. Step response of the PID closed-loop control.

3.2. FLC

FLC is typically composed of four elements: i) fuzzification inference, ii) knowledge-based fuzzy rules, iii) Inference engine or decision making and iv) defuzzification inference [5, 30]. The fuzzification inference section determines the input variables and transforms them into fuzzy representation. The fuzzy rule base part contains the expert-defined rules required to produce the output. Hence, the fuzzified values are processed, by the inference engine,

using the rule base which consists of IF-THEN rules known as fuzzy rules [24]. The defuzzification part converts the fuzzy quantities into crisp values at the output. The block diagram of a general FLC is shown in Fig. 5.

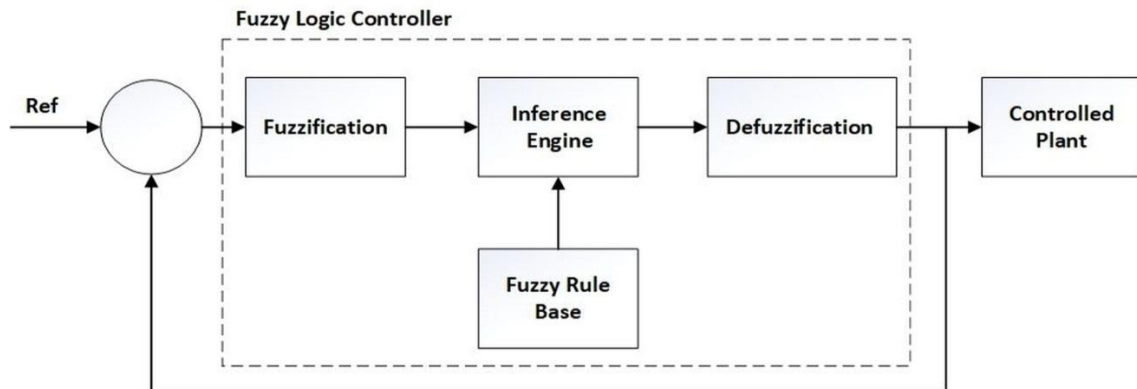


Fig. 5. Block diagram of the general FLC.

In this section, FLC controller is utilized to control the output voltage of the AVR system according to the error signal resulted from comparing a unity step reference input signal with the actual feedback output voltage. The PD-like FLC (Mamdani type) has two inputs and one output. The FLC inputs represent the error and change of error, while the output forms the control action applied to the system to track a desired reference signal. The two inputs are normalized by scaling factors K_1 and K_2 before being fuzzified. The normalized inputs/output are fuzzified by a fuzzy set of five equally distributed triangular membership functions with 50% overlap. The fuzzy output, resulting from the fired fuzzy rules, is converted to crisp value using the centre of area defuzzification method. The output is then scaled by a scaling factor (K_3). The input and output membership functions of the FLC can be seen in Fig. 6. A standard PD-like fuzzy rule base, of 25 rules, is used as shown in Table 1, in which NB, NM, NS, Z, PS, PM and PB denote negative big, negative medium, negative small, zero, positive small, positive medium and positive big, respectively. The FLC closed-loop approach is presented in Fig. 7.

Table 1. Fuzzy rules.

e / Δe	Δe	NB	NS	Z	PS	PB
NB		NB	NB	NB	NS	Z
NS		NB	NB	NS	Z	PS
Z		NB	NS	Z	PS	PB
PS		NS	Z	PS	PB	PB
PB		Z	PS	PB	PB	PB

The input and output scaling factors of the FLC are tuned using GA to obtain minimum overshoot and minimum SSE. The values of the scaling factors obtained are: $K_1=3.1$, $K_2=0.9$ and $K_3=1.4$.

3.2.1. Results

The step response of the fuzzy logic control approach is exhibited in Fig. 8, from which it is clear that the system is stable. The delay time (T_d) is 0.49 s, rise time (T_r) is 0.89 s, the

settling time (T_s) is 2.20 s and SSE is 0.016 V. The reason behind the SSE is the absence of integral action in the PD-like FLC that is necessary to eliminate the SSE.

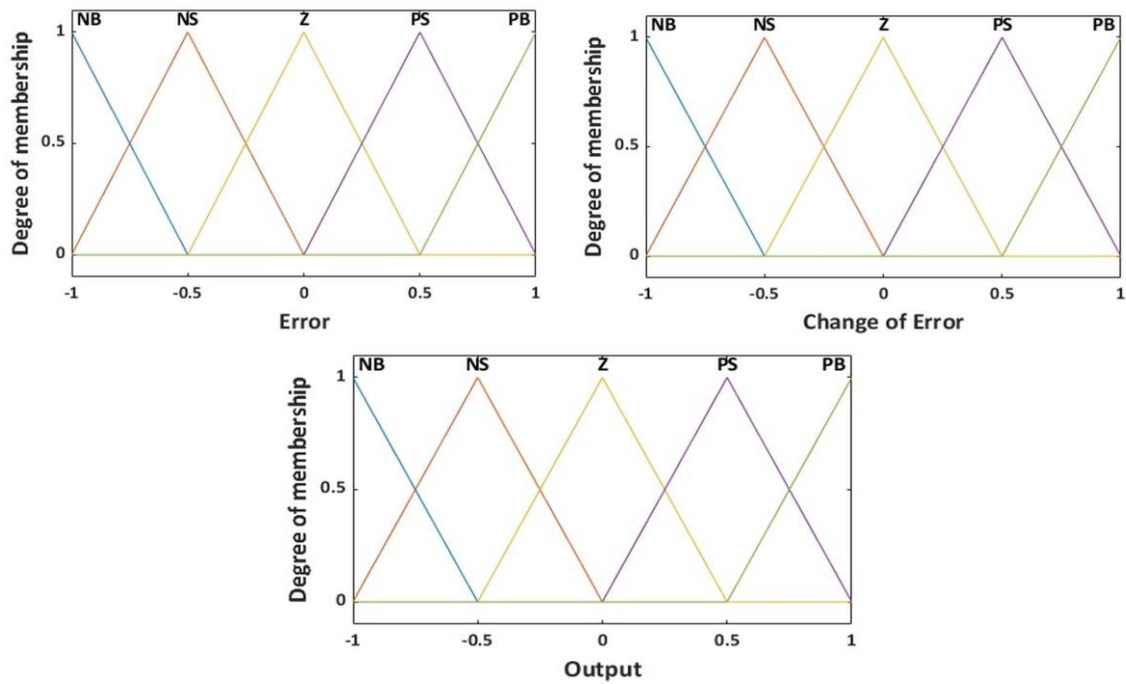


Fig. 6. Input/Output membership functions of the FLC.

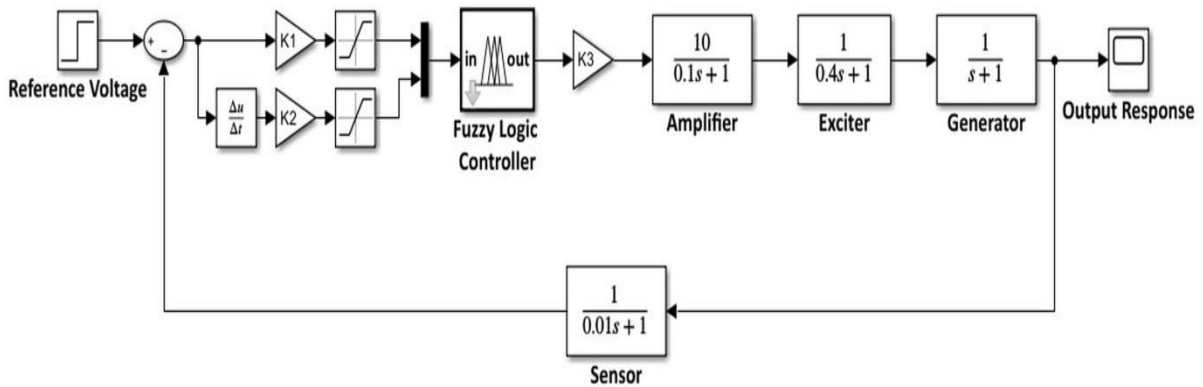


Fig. 7. The closed-loop control approach using FLC.

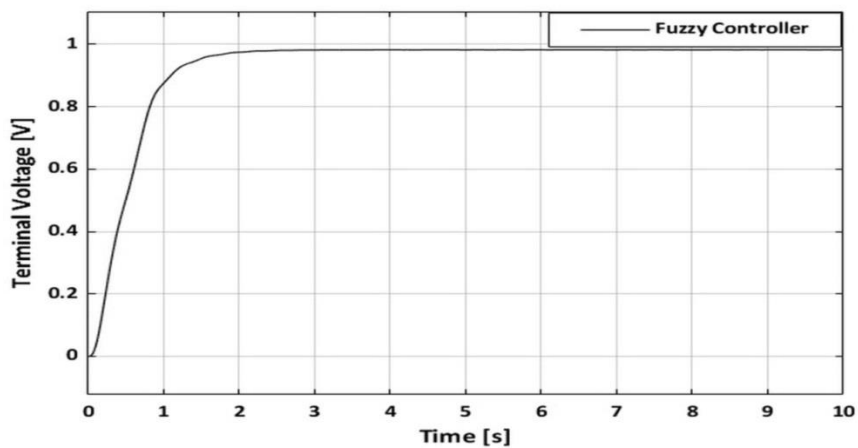


Fig. 8. Step response of the FLC closed-loop control.

3.3. ANFIS Controller

3.3.1. ANFIS Network Architecture

The architecture of a general ANFIS network can be seen in Fig. 9. The structure of the network can be varied according to the number of inputs and membership functions; however, it permanently consists of 5 layers. The nodes at the same layer coincide with the same family of functions, as explained below [29].

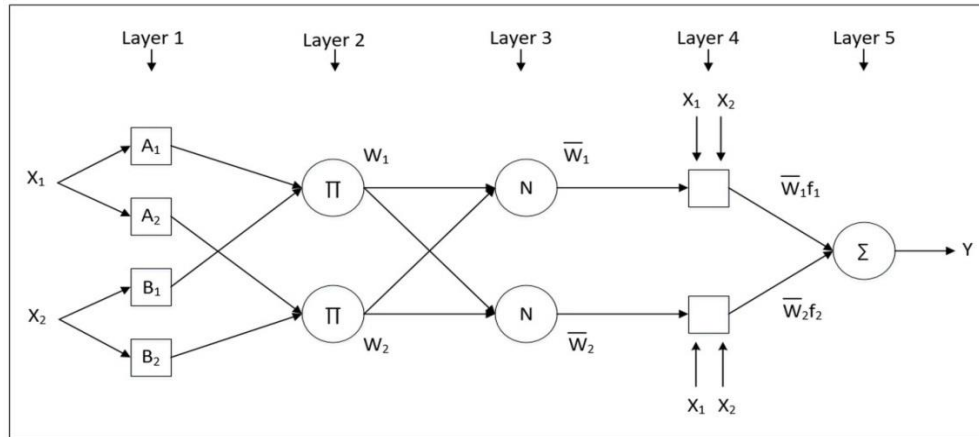


Fig. 9. General structure of an ANFIS network.

- **Layer 1:** This layer converts the input data into fuzzy logic values. In this layer, the node function is a membership function O_i^1 of the function A_i and is described as [29]:

$$O_i^1 = \mu_{A_i}(x) = e^{-\left(\frac{x-c_i}{s_i}\right)^2} \quad (7)$$

where x is the input value at node (i), A_i is the related linguistic tag, while $\mu_{A_i}(x)$ is a Gaussian function with a value ranging between 0 and 1. The parameters c_i and s_i are called the set of premise parameters, and are altered by the learning algorithm of the ANFIS network.

- **Layer 2:** In this layer the activation of each one of the rules is performed. The output of this layer is the product of the input values, described as [29]:

$$O_i^2 = w_i = \mu_{A_i}(x) \mu_{B_i}(x), \quad i = 1, 2 \quad (8)$$

- **Layer 3:** In this layer, the activation signals of fuzzy rules are normalized by the following formula [29]:

$$O_i^3 = \bar{w}_i = \frac{w_i}{w_1 + w_2}, \quad i = 1, 2 \quad (9)$$

- **Layer 4:** In this layer, the weighted consequent parameters are computed using the IF-THEN rules of Takagi-Sugeno-Kang (TSK) function, as shown by the following formula [29]:

$$O_i^4 = \bar{w}_i f_i = \bar{w}_i (a_1 x_1 + a_2 x_2 + a_3), \quad i = 1, 2 \quad (10)$$

where \bar{w}_i is the output of the previous layer, i.e. layer 3, and f_i is the TSK function. This function consists of a set of consequent parameters (a_1, a_2, a_3) that are also modified and adjusted by the ANFIS network during the training process.

- **Layer 5:** In this layer, the total output of the ANFIS network is calculated as a weighted average of all input values to its node, as described below [29]:

$$O_i^4 = y = \frac{\sum_{i=1}^2 \bar{w}_i f_i}{\sum_{i=1}^2 \bar{w}_i}, \quad i = 1, 2 \quad (11)$$

3.3.2. ANFIS Controller for the AVR System

In this section, an ANFIS controller is built and utilized to control the AVR system in a closed-loop control approach. The neuro-fuzzy designer toolbox in Matlab/Simulink software is used to build the ANFIS controller. The input and output data (312 readings) of the tuned PID controller used in the previous section, is recorded and used to train the ANFIS model. To generate the FIS file, grid partition method is selected as the ANFIS controller has single input and single output. Also, for the input membership function of the FIS, 10 Gaussian membership functions are used with linear membership function for the output to increase the flexibility of the controller and obtain better results. To train the FIS file, hybrid optimization method with 100 Epochs is used. The training and the structure of the ANFIS model can be seen in Figs. 10 and 11, respectively. Also, the closed-loop control approach using ANFIS controller is shown in Fig. 12.

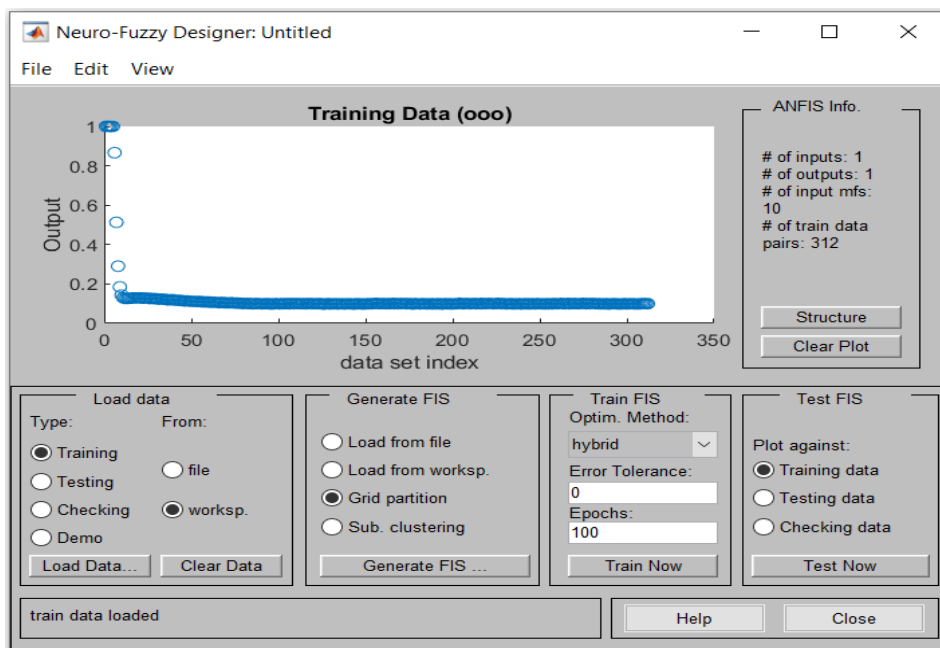


Fig. 10. Training of the ANFIS controller.

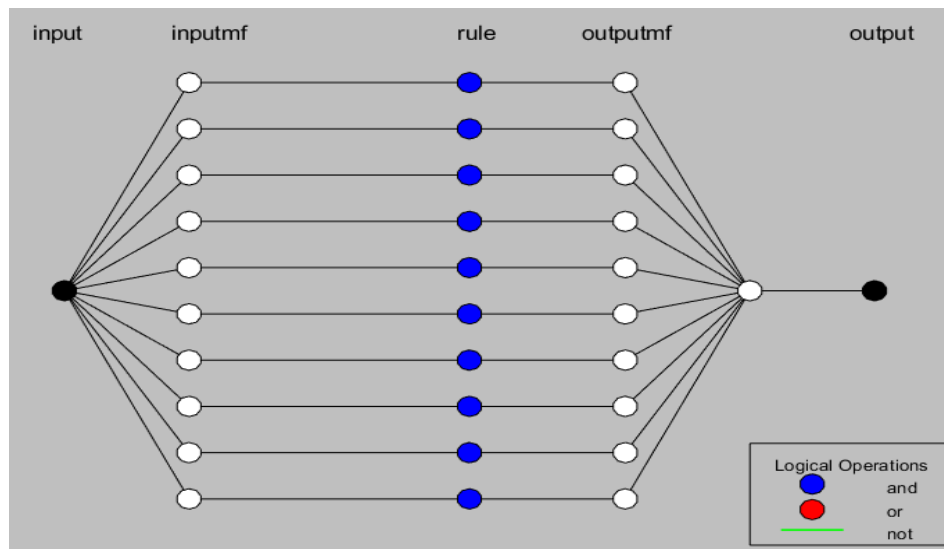


Fig. 11. Structure of the ANFIS controller.

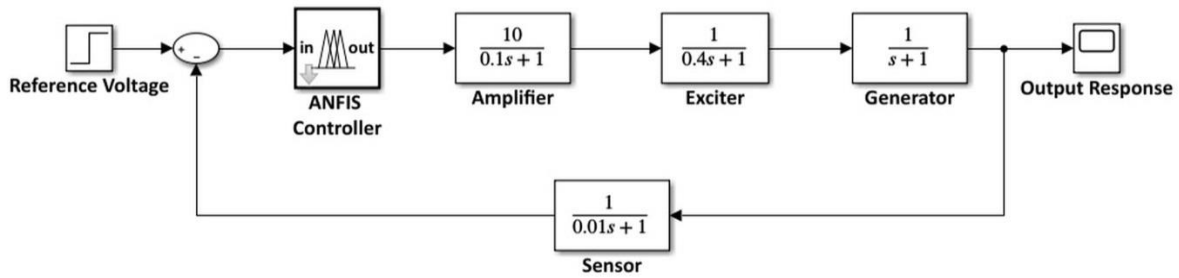


Fig. 12. Closed-loop control approach using the ANFIS controller.

The step response of the closed-loop control approach using the ANFIS controller is depicted in Fig. 13. It is clear that the system is stable and the controller was successful in controlling the terminal voltage and tracking the step reference voltage. The delay time (T_d) is 0.66 s, rise time (T_r) is 1.27 s, the settling time (T_s) is 3.10 s and the SSE is 0 V.

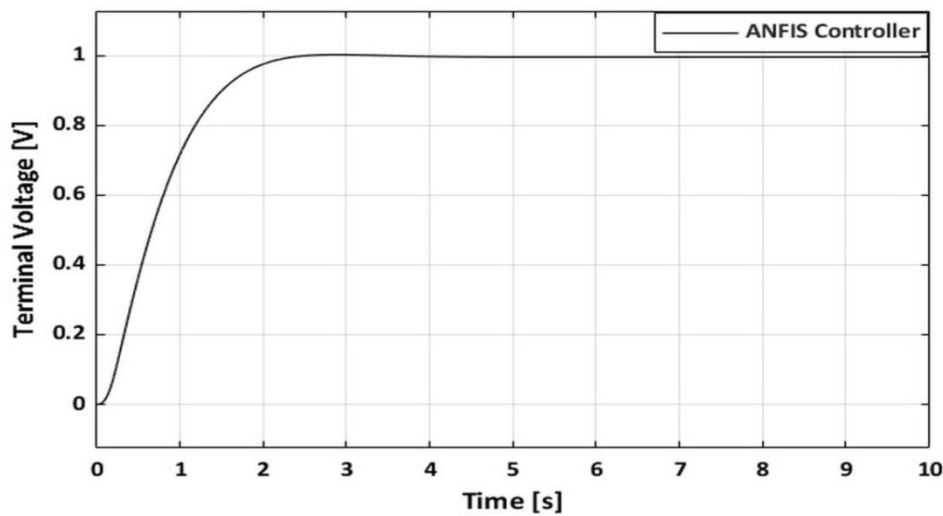


Fig. 13. The step response of the system using ANFIS controller.

To compare the performance of the PID, FLC and ANFIS controllers, the step response - of the closed-loop control approach using these controllers - is recorded and depicted in Fig. 14. Also, the time response specifications using the three controllers is shown in Table 2.

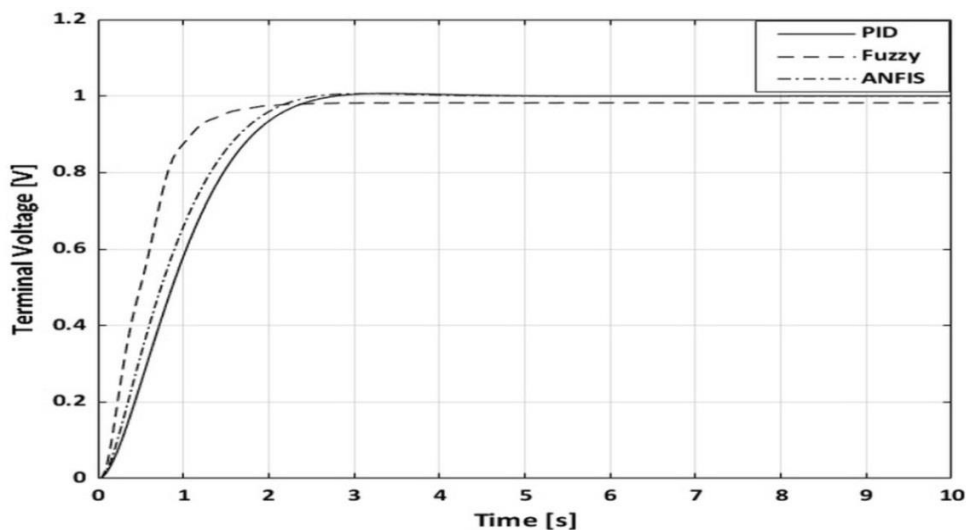


Fig. 14. Step response of the system using PID, FLC and ANFIS controllers.

Table 2. Time response specification using the PID, FLC and ANFIS.

Controller	Delay time [s]	Rise time [s]	Settling time [s]	Peak overshoot [%]	Peak value	Peak time [s]	SSE [V]
PID	0.87	1.54	3.50	0.66	1.0066	3.25	0
FLC	0.49	0.89	2.20	-	-	-	0.016
ANFIS	0.66	1.27	3.10	0.27	1.0027	2.88	0

It's obvious from Fig. 14 and Table 2 that FLC controller produces a faster response (minimal delay, rise and settling times) with zero overshoot. However, the SSE is respectively high as compared to other controllers. This is because the PD-like FLC lacks the integral term that is responsible for eliminating the SSE. The ANFIS controller has produced zero SSE with faster performance than the PID in terms of delay and rise times. Also, the ANFIS controller reduced the overshoot as compared with that of the PID controller.

4. DISTURBANCE REJECTION OF THE CONTROLLERS

To test the ability of the controllers to resist and reject unexpected disturbance signals, positive and negative signals are applied at the time interval lying between 4 s and 5 s, to the system as shown in Fig. 15. The performance of each controller is recorded as shown in Fig. 16.

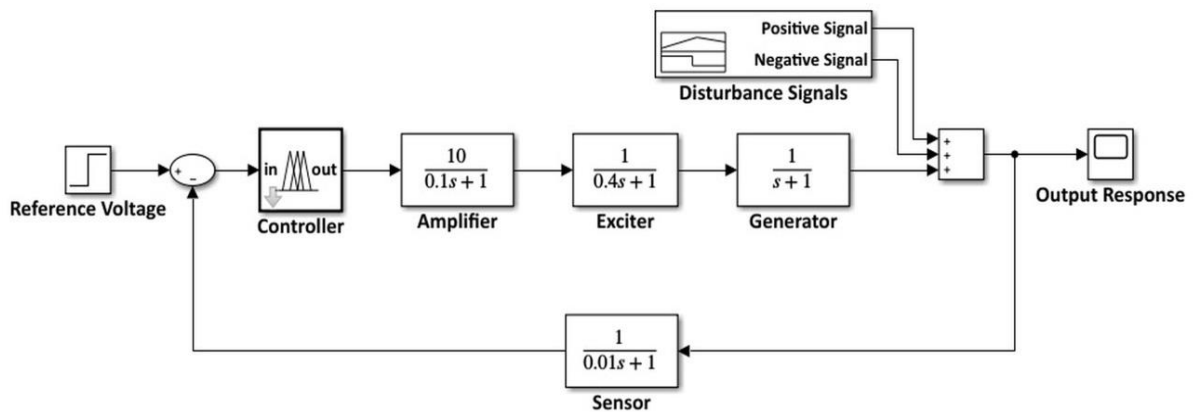


Fig. 15. The closed-loop control with positive and negative disturbance signals.

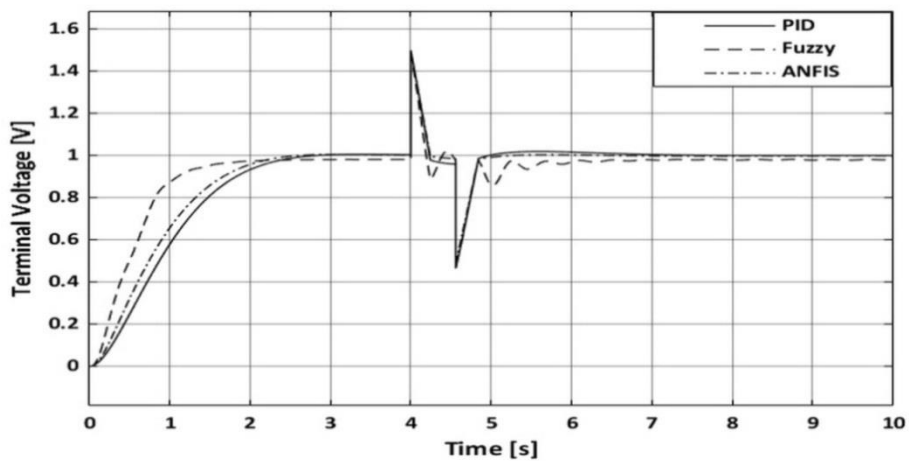


Fig. 16. Step response of the system with positive and negative disturbance signals using PID, FLC and ANFIS controllers.

It is clear from Fig. 16 that the three controllers were able to reject the disturbance signals and managed to track the reference voltage signal. However, the FLC was not robust enough as it produced some fluctuation in the output for more than 1s before it settled down. Also, it can be seen from the figure that the PID controller has produced a slight overshoot, during the time interval lying between 5 s and 7 s, after receiving the negative disturbance signal, while the ANFIS controller has successfully rejected both the positive and negative disturbance signals and produced stable control performance.

5. ROBUSTNESS OF THE CONTROLLERS

Sudden and unexpected changes in system parameters may lead to vital problems due to dealing with kilo volts as an output of the system. For this reason, it is important to test the robustness of the controller against any possible changes in system parameters. In this section, the performance of the three mentioned controllers are tested against changes in the time constant of the amplifier (τ_a), the exciter (τ_e), the generator (τ_g) and the sensor (τ_s) of the system. The range of changes in the parameters is selected as $\pm 50\%$ of the original value in steps of $\pm 25\%$. The time response of each controller is shown in Tables 3, 4 and 5.

Table 3 reveals that the PID controller produced large values in the overshoot (MP) and an increase in the settling time (Ts). The time delay (Td) and settling time (Ts) are almost stable. Although the SSE is remained zero - which shows the ability of the controller to successfully track the desired reference voltage in the steady state - the large increase in the overshoot may lead to serious problems due to dealing with high voltages.

Table 3. Time response of the PID controller using different system parameters.

Parameter	Change in parameter [%]	Peak overshoot [%]	Time delay [s]	Rise time [s]	Settling time [s]	SSE [V]
τ_a	+50	1.60	0.95	1.47	3.80	0
	+25	1.07	0.89	1.51	3.80	0
	-25	21.30	0.85	1.59	4.50	0
	-50	13.80	0.84	1.63	4.50	0
τ_e	+50	5.45	0.99	1.52	4.50	0
	+25	2.90	0.94	1.52	4.10	0
	-25	0.00	0.80	1.64	3.30	0
	-50	0.00	0.73	1.80	3.70	0
τ_g	+50	7.50	1.07	1.76	6.00	0
	+25	4.30	0.97	1.62	5.20	0
	-25	0.00	0.75	1.51	4.50	0
	-50	0.00	0.62	1.96	5.50	0
τ_s	+50	0.72	0.87	1.53	3.20	0
	+25	0.69	0.87	1.54	3.20	0
	-25	0.63	0.87	1.56	3.20	0
	-50	0.60	0.87	1.55	3.20	0

In contrast, it is clear from Table 4 that the FLC controller has a stable performance with different system parameters, i.e., stable Td, Ts and Tr, together with a slight increase in SSE amounting to 12.5% of the original value. Although, the increase in the SSE looks small, its

value is considered a large one as dealing with kilo volts at the output. Also, from Table 5, it can be seen that the ANFIS controller showed almost a stable performance, i.e., stable Td, Ts and Tr, with different system parameters. However, it slightly suffers from an increase in the overshoot. Nonetheless, it successfully managed to keep the SSE at zero within a short time. The increase in the overshoot is relatively small as compared with that of the PID.

Table 4. Time response of the FLC controller using different system parameters.

Parameter	Change in parameter [%]	Peak overshoot [%]	Time delay [s]	Rise time [s]	Settling time [s]	SSE [V]
τ_a	+50	0	0.48	0.97	2.00	0.018
	+25	0	0.49	0.97	1.80	0.018
	-25	0	0.51	0.93	1.80	0.018
	-50	0	0.51	0.94	2.00	0.018
τ_e	+50	0	0.54	0.94	2.00	0.018
	+25	0	0.52	0.97	1.90	0.018
	-25	0	0.47	0.90	1.80	0.018
	-50	0	0.45	0.90	1.90	0.018
τ_g	+50	0	0.57	0.96	2.00	0.018
	+25	0	0.54	0.96	2.00	0.018
	-25	0	0.45	0.90	2.20	0.018
	-50	0	0.38	0.82	2.20	0.018
τ_s	+50	0	0.47	0.95	1.80	0.018
	+25	0	0.48	0.93	1.90	0.018
	-25	0	0.51	0.93	2.20	0.018
	-50	0	0.52	0.92	2.20	0.018

Table 5. Time response of the ANFIS controller using different system parameters.

Parameters	Change in parameter [%]	Peak overshoot [%]	Time delay [s]	Rise time [s]	Settling time [s]	SSE [V]
τ_a	+50	0.91	0.76	1.38	3.10	0
	+25	0.75	0.75	1.39	3.10	0
	-25	0.49	0.73	1.42	3.10	0
	-50	0.39	0.73	1.48	3.10	0
τ_e	+50	1.36	0.88	1.62	3.80	0
	+25	1.05	0.80	1.50	3.80	0
	-25	0.16	0.67	1.39	3.00	0
	-50	0.00	0.60	1.37	3.00	0
τ_g	+50	0.00	0.97	2.10	3.50	0
	+25	0.17	0.85	1.75	3.00	0
	-25	1.40	0.63	1.15	3.00	0
	-50	2.40	0.51	0.88	2.80	0
τ_s	+50	0.64	0.73	1.42	3.20	0
	+25	0.63	0.73	1.42	3.20	0
	-25	0.60	0.75	1.44	3.20	0
	-50	0.58	0.76	1.47	3.20	0

6. CONCLUSIONS AND FUTURE WORK

In this research work, three different controllers, namely PID, PD-like FLC and ANFIS are used to control an AVR system. The performance of the three controllers was recorded and analyzed. Although the FLC was better than other controllers in terms of delay and rising times, and produced a zero overshoot in the output, but the FLC produced a steady-state error of 0.016 V and was not robust enough to disturbances as it produced fluctuations for almost 2 s when exposed to negative disturbance signal. The ANFIS controller was faster than PID controller in terms of delay and rising times, and produced less overshoot compared with the PID. The ANFIS controller showed superior performance in rejecting positive and negative disturbance signals compared to the other two controllers. In terms of robustness to changes in system parameters, both FLC and ANFIS showed a good performance. However, the FLC suffered from 12.5% increase in the SSE, whereas the ANFIS controller managed to keep the SSE to zero with a slight increase in the overshoot in some cases. The PID controller suffered from large overshoot values in some cases. Based on the aforesaid, it can be concluded that the ANFIS controller is more suitable and reliable than PD-like FLC and PID controllers and can be used in an AVR system. This is due to its ability to both produce a zero SSE and resist unexpected disturbance signals and/or unexpected changes in system parameters. As a future work, an integral action can be added to the PD-like FLC to be compared with the performance of PID and ANFIS controllers. Also, the performance of the controllers can be tested with real synchronous generator connected to a 230 kV network in a simulation environment.

REFERENCES

- [1] M. Sahib, "A novel optimal PID plus second order derivative controller for AVR system," *Engineering Science and Technology, an International Journal*, vol. 18, no. 2, pp. 194-206, 2015.
- [2] M. Ayas, E. Sahin, "FOPID controller with fractional filter for an automatic voltage regulator," *Computers and Electrical Engineering*, vol. 90, pp. 106895, 2021.
- [3] M. Soliman, M. Ali, "Parameterization of robust multi-objective PID-based automatic voltage regulators: generalized Hurwitz approach," *International Journal of Electrical Power and Energy Systems*, vol. 133, pp. 107216, 2021.
- [4] H. Zhang, F. Shi, Y. Liu, "Enhancing optimal excitation control by adaptive fuzzy logic rules," *International Journal of Electrical Power and Energy Systems*, vol. 63, pp. 226-235, 2014.
- [5] Y. Lin, "Proportional plus derivative output feedback based fuzzy logic power system stabiliser," *International Journal of Electrical Power and Energy Systems*, vol. 44, no. 1, pp. 301-307, 2013.
- [6] B. ChristyJuliet, D. Vinothini, S. Vidhyashree, "Power system stabilisation based on Ga-Anfis in generators," *International Journal of Research in Engineering and Technology*, vol. 3, no. 7, pp. 758-760, 2014.
- [7] M. Elsis, M. Tran, H. Hasanien, R. Turky, F. Albalawi, S. Ghoneim, "Robust model predictive control paradigm for automatic voltage regulators against uncertainty based on optimization algorithms," *Mathematics*, vol. 9, no. 22, pp. 2885, 2021.
- [8] M. Modabbernia, B. Alizadeh, A. Sahab, M. Moghaddam, "Robust control of automatic voltage regulator (AVR) with real structured parametric uncertainties based on H_∞ and μ -analysis," *ISA Transactions*, vol. 100, pp. 46-62, 2020.

- [9] M. Elsis, "Design of neural network predictive controller based on imperialist competitive algorithm for automatic voltage regulator," *Neural Computing and Applications*, vol. 31, pp. 5017-5027, 2019.
- [10] A. Sikander, P. Thakur, "A new control design strategy for automatic voltage regulator in power system," *ISA Transactions*, vol. 100, pp. 235-243, 2020.
- [11] M. Elsis, M. Soliman, "Optimal design of robust resilient automatic voltage regulators," *ISA Transactions*, vol. 108, pp. 257-268, 2021.
- [12] Y. Tang, L. Zhao, Z. Han, X. Bi, X. Guan, "Optimal gray PID controller design for automatic voltage regulator system via imperialist competitive algorithm," *International Journal of Machine Learning and Cybernetics*, vol. 7, no. 2, pp. 229-240, 2016.
- [13] A. Sikander, P. Thakur, R. Bansal, S. Rajasekar, "A novel technique to design cuckoo search based FOPID controller for AVR in power systems," *Computers and Electrical Engineering*, vol. 70, pp. 261-274, 2018.
- [14] X. Li, Y. Wang, N. Li, M. Han, Y. Tang, F. Liu, "Optimal fractional order PID controller design for automatic voltage regulator system based on reference model using particle swarm optimization," *International Journal of Machine Learning and Cybernetics*, vol. 8, no. 5, pp. 1595-1605, 2017.
- [15] A. Al Gizi, M. Mustafa, N. Al-geelani, M. Alsaedi, "Sugeno fuzzy PID tuning, by genetic-neutral for AVR in electrical power generation," *Applied Soft Computing*, vol. 28, pp. 226-236, 2015.
- [16] V. Mukherjee, S. Ghoshal, "Intelligent particle swarm optimized fuzzy PID controller for AVR system," *Electric Power Systems Research*, vol. 77, no. 12, pp. 1689-1698, 2007.
- [17] A. Al Gizi, "A particle swarm optimization, fuzzy PID controller with generator automatic voltage regulator," *Soft Computing*, vol. 23, pp. 8839-8853, 2019.
- [18] P. Dabur, N. Yadav, R. Avtar, "Matlab design and simulation of AGC and AVR for single area power system with fuzzy logic control," *International Journal of Soft Computing and Engineering*, vol. 1, no. 6, pp. 44-49, 2012.
- [19] K. Yavarian, A. Mohammadian, F. Hashemi, "Adaptive neuro fuzzy inference system PID controller for AVR system using SNR-PSO optimization," *International Journal on Electrical Engineering and Informatics*, vol. 7, no. 3, pp. 394-408, 2015.
- [20] N. Pachauri, "Water cycle algorithm-based PID controller for AVR," *The International Journal for Computation and Mathematics in Electrical and Electronic Engineering*, vol. 39, no. 3, pp. 551-567, 2020.
- [21] K. Yavarian, F. Hashemi, A. Mohammadian, "Design of intelligent PID controller for AVR system using an adaptive neuro fuzzy inference system," *International Journal of Electrical and Computer Engineering*, vol. 4, no. 5, pp. 703-718, 2014.
- [22] P. Govindan, "Evolutionary algorithms-based tuning of PID controller for an AVR system," *International Journal of Electrical and Computer Engineering*, vol. 10, no. 3, pp. 3047-3056, 2019.
- [23] A. Aboelhassan, M. Abdelgeliel, E. Zakzouk, M. Gale, "Design and implementation of model predictive control based PID controller for industrial applications," *Energies*, vol. 13, no. 24, pp. 6594, 2020.
- [24] R. Precup, H. Hellendoorn, "A survey on industrial applications of fuzzy control," *Computers in Industry*, vol. 62, pp. 213-226, 2011.
- [25] H. Chaudhary, S. Khatoun, R. Singh, "ANFIS based speed control of DC motor," *Proceedings of IEEE Symposium Series on Innovative Applications of Computational Intelligence on Power, Energy and Controls with their Impact on Humanity*, pp. 63-67, 2016.
- [26] T. Spoljaric, C. Lusetic, V. Simovic, "Optimization of PID controller in AVR system by using ant lion optimizer algorithm," *MIPRO*, pp. 1522-1526, 2018.

- [27] V. Nath, D. Sambariya, "Analysis of AGC and AVR for single area and double area power system Using fuzzy logic control," *International Journal of Advanced Research in Electrical, Electronics and Instrumentation Engineering*, vol. 4, no. 7, 2015.
- [28] C. Rao, K. Sahu, S. Yellampalli, B. Rao, "Performance of a fuzzy logic based AVR in SMIB, MMIB system and power flow control using SSSC and IPFC," *International Journal of Engineering Research and Applications*, vol. 2, no. 1, pp. 260-268, 2012.
- [29] R. Pérez, F. Rodríguez, D. Vega, "Design of an ANFIS automatic voltage regulator of a synchronous generator," *Proceedings of IEEE International Autumn Meeting on Power, Electronics and Computing*, pp. 1-6, 2020.
- [30] V. Nath, D. Sambariya, "Analysis of AGC and AVR for single area and double area power system using fuzzy logic control," *International Journal of Advanced Research in Electrical, Electronics and Instrumentation Engineering*, vol. 4, pp. 6501-6511, 2015.